

## Superradiant Droplet Emission from Parametrically Excited Cavities

Valeri Frumkin\* and John W. M. Bush<sup>†</sup>

Department of Mathematics, Massachusetts Institute of Technology

Konstantinos Papatryfonos<sup>‡\*</sup>Department of Mathematics, Massachusetts Institute of Technology, Cambridge, Massachusetts 02139, USA  
and Gulliver UMR CNRS 7083, ESPCI Paris, Université PSL, 75005 Paris, France (Received 5 May 2022; accepted 23 December 2022; published 9 February 2023)

Superradiance occurs when a collection of atoms exhibits a cooperative, spontaneous emission of photons at a rate that exceeds that of its component parts. Here, we reveal a similar phenomenon in a hydrodynamic system consisting of a pair of vibrationally excited cavities, coupled through their common wave field, that spontaneously emit droplets via interfacial fracture. We show that the droplet emission rate of two coupled cavities is higher than the emission rate of two isolated cavities. Moreover, the amplified emission rate varies sinusoidally with distance between the cavities, as is characteristic of superradiance. We thus present a hydrodynamic phenomenon that captures several essential features of superradiance in optical systems.

DOI: [10.1103/PhysRevLett.130.064002](https://doi.org/10.1103/PhysRevLett.130.064002)

When a group of  $N$  quantum emitters (e.g., excited atoms) interact coherently with a common electromagnetic field, they may collectively emit photons at a rate that is proportional to  $N^2$  [1,2]. In quantum optics, this phenomenon is known as superradiance [3], an effect of both fundamental and practical interest, with applications in various fields, including quantum information technologies [4–6], cryptography [7], and narrow linewidth lasers [8–10]. When the emitters are separated by less than a wavelength, this situation requires the emitters to radiate with the same phase [3]. When they are separated by distances comparable to or greater than the wavelength, each emitter must radiate with the local phase of the mode into which they emit [11–13]. In the case of coherently driven emitters, the atomic coherence, and thus the phase of the radiated field, is set by the local phase of the drive field. The phase-matching condition then leads to a sinusoidal modulation of the spontaneous emission rate versus the emitter spacing [14]. This modulation was first demonstrated using a pair of trapped ions whose separation distance  $d$  was varied gradually [15]. Experiments revealed sinusoidal oscillations of the spontaneous emission rate  $\Gamma_{\text{sp}}$  of the two-ion crystal, in accord with detailed quantum mechanical theoretical analysis [16]. This type of superradiance was first considered to be a purely quantum phenomenon [15,16], but has since been rationalized in terms of classical electromagnetic theory [17].

Fluid mechanics has produced laboratory-scale physical analogs for phenomena as disparate as the wave nature of light [18], black holes [19], the Casimir effect [20], the Aharonov-Bohm effect [21], and the periodic table [22]. The relatively recent discovery of a pilot-wave

hydrodynamic system [23] has led to a new class of hydrodynamic quantum analogs [24] that includes analogs of quantized orbital states [25,26], quantum corrals [27,28], Friedel oscillations [29], and spin lattices [30].

We here show that superradiance can also be seen in a hydrodynamic setting. We consider a system of vibrationally excited hydrodynamic cavities that spontaneously emit droplets via interfacial fracture. The cavities are deep circular wells spanned by a thin layer of oil that allows for their coupling through a common wave field (see Fig. 1). We demonstrate that the wave field in each cavity is influenced by the presence of its neighbor. Specifically, the neighboring cavity may amplify the local oscillation amplitude, resulting in an increased chance of interfacial fracture and thus an amplified droplet emission rate.

Figure 1 shows a schematic representation of our experimental setup. A bath of fluorinated oil has two 6-mm-deep circular wells that serve as hydrodynamic cavities. The cavities, each with diameter 7 mm, are separated by a center-to-center distance  $d$  that is varied between experiments, from 8 mm to 12 mm, in 0.5-mm increments. In the shallow layer spanning the wells, the depth is  $0.75 \pm 0.05$  mm. The system is subjected to vertical vibration by an electromagnetic shaker with forcing  $\ddot{z} = \gamma \cos(\delta t)$ , where  $\gamma \approx 1.75$  g and  $f \approx 39$  Hz are the peak driving acceleration and frequency, respectively. A more detailed description of the experimental setup is provided in the Supplemental Material [31], which includes Ref. [32].

A liquid bath of uniform depth subject to vertical vibration at a fixed frequency undergoes two critical transitions as the driving amplitude is increased progressively. The first

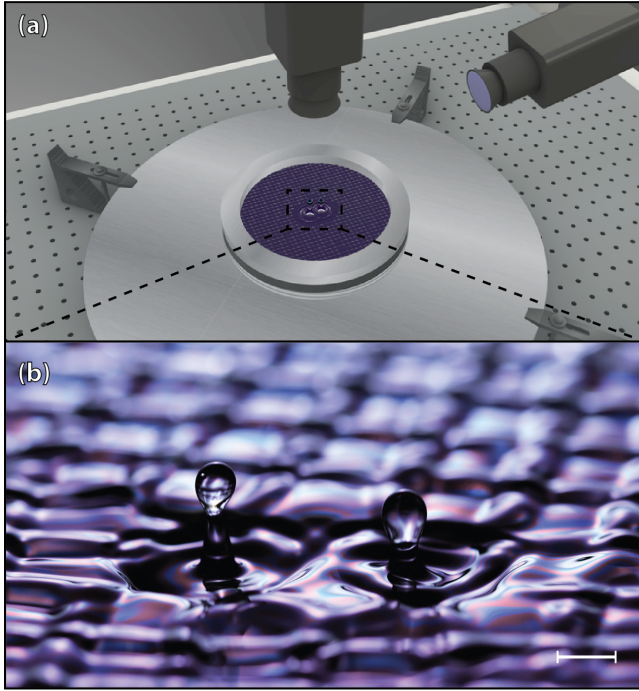


FIG. 1. The experimental setup (see also Supplemental Material, Fig. 1 [31]). (a) A schematic illustration of a circular bath with two cavities spanned by a thin layer of fluorinated oil. The bath is vertically oscillated by an electromagnetic shaker, resulting in the emission of droplets from the two cavities. (b) A rare generation event in which two droplets are about to be created simultaneously. Scale bar, 3 mm.

transition occurs as the vibrational acceleration,  $\gamma \approx 4\pi^2 f^2 A$ , where  $A$  is the vibration amplitude, is increased beyond the Faraday threshold,  $\gamma_F$ , at which point the initially flat free surface destabilizes into a pattern of standing Faraday waves [33]. As the driving amplitude is increased further, the stabilizing influence of surface tension is exceeded by the destabilizing inertial forces associated with the bath vibration, and the interfacial fracture threshold  $\gamma_B$  is crossed. Above this threshold, the Faraday waves break spontaneously, and millimetric droplets are emitted from the free surface in an irregular fashion [34,35]. Importantly, for shallow layers, both  $\gamma_F$  and  $\gamma_B$  depend strongly on the local depth of the liquid. We thus define  $\gamma_F^c$  and  $\gamma_F^s$  to be the Faraday threshold above the cavities and the shallow region, respectively, and likewise for  $\gamma_B$ .

With the increase of the driving acceleration  $\gamma$ , our variable-depth system undergoes the following evolution. First, as the acceleration crosses  $\gamma_F^c$ , Faraday waves appear above the cavities and propagate some distance into the surrounding shallow region. When  $\gamma > \gamma_F^s$ , Faraday waves emerge over the entirety of the bath surface, but are most vigorous above the cavities. Figure 2 illustrates the instantaneous wave field near the cavities when  $\gamma_F^c < \gamma < \gamma_B^c$ . Figure 2(a) shows the wave field of a single cavity, whereas Figs. 2(b)–2(d) show the two-cavity wave field for three

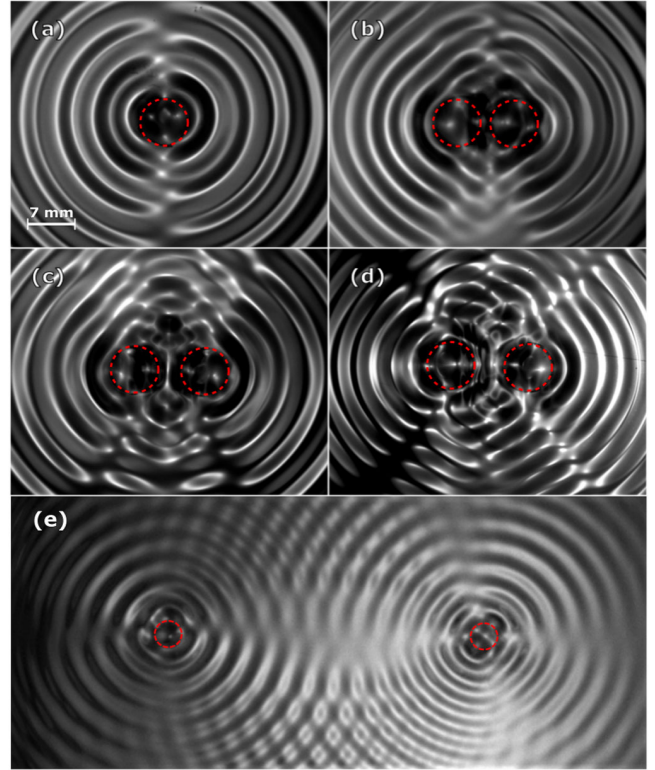


FIG. 2. Images of the instantaneous wave field generated by the cavities (red circles). (a) A single cavity. Two cavities with center-to-center distances of (b)  $d \approx 8$  mm, (c)  $d \approx 10.5$  mm, (d)  $d \approx 12$  mm, and (e)  $d \approx 87$  mm.

different values of the center-to-center separation distance,  $d \approx 8, 10.5, 12$  mm, respectively. Figure 2(e) depicts the resulting wave field for two distant cavities, with  $d \approx 87$  mm. Notably, even at such large separation distances, the perturbation wave field can reach the other cavity, allowing for long-range interactions. The perturbation wave field, recorded near the frequency of the most unstable Faraday mode,  $f=2$ , is shown in the Supplemental Material, Movie 1 [31].

When the acceleration is increased beyond the interfacial breaking threshold of the cavities,  $\gamma_B^c < \gamma < \gamma_B^s$ , droplet emission sets in. Movie 2 in the Supplemental Material [31] shows the spontaneous droplet emission from a pair of hydrodynamic cavities. The emission events occur unpredictably, as indicated by Fourier analysis shown in the Supplemental Material [31], but arise exclusively within the cavities. We define a spontaneous emission rate  $\Gamma$  for the combined two-cavity system, as the average number of emission events per second, and the anomalous emission rate,  $\Gamma_N \delta d \approx \frac{1}{2} \Gamma \delta d - 2\Gamma_0 = 2\Gamma_0$ , where  $\Gamma_0 \approx 1.47 \text{ s}^{-1}$  is the measured emission rate of a single cavity in isolation.

In Fig. 3(a), we present our experimental measurements of the dependence of the anomalous emission rate  $\Gamma_N \delta d$  on the separation distance  $d$ . An amplification of up to 46% relative to  $2\Gamma_0$  is evident. One expects the emission rate to

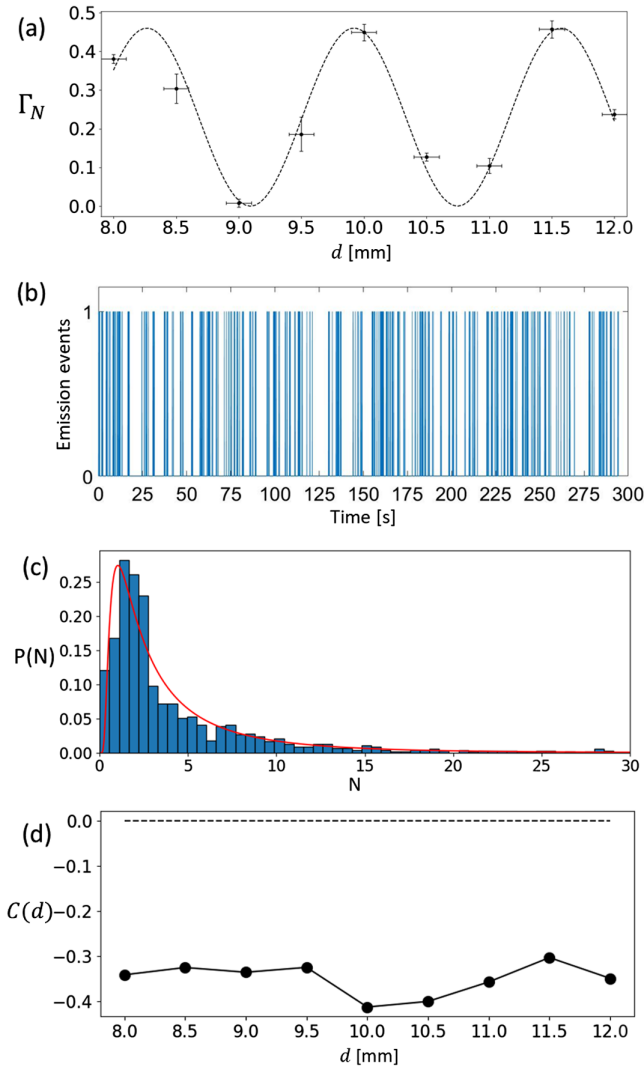


FIG. 3. Experimental measurements of the droplet emission rate. (a) Dependence of the anomalous emission rate,  $\Gamma_N \delta d \approx \Gamma_0 \delta d - 2\Gamma_0$  (black dots) on center-to-center intercavity distance  $d$ . Each data point represents an average over a time interval of 300 seconds, corresponding to roughly 950–1300 droplet emission events. The dashed curve represents  $A \cos^2 \delta 2kd$ , with  $A \approx 1.36$  and  $k \approx 0.85 \text{ mm}^{-1}$  being the experimentally measured Faraday wave number in the vicinity of the cavities. (b) Time series of the emission events from a single cavity over a 300-second interval indicates the unpredictability of a single emission event. (c) Histogram of the interemission time intervals and its comparison to the first passage time model [36]. The red curve represents an inverse Gaussian distribution as given by Eq. (2). (d) Measured correlation  $C$  of the drop emission event in the two cavities as a function of their separation distance  $d$ . The upper dashed line represents two uncorrelated cavities.

be a function of the kinetic energy of the fluid inside the cavity. For an isolated cavity, the average kinetic energy per oscillation period is constant, corresponding to a steady emission rate  $\Gamma_0$ . In the presence of a second, coupled cavity, the wave field inside each cavity is effected by its neighbor, and the average kinetic energy per oscillation

period will depend on the distance between the two. As in the trapped ion pair experiment [15], the amplified emission rate of our two-cavity system oscillates sinusoidally as a function of the distance between the cavities. The observed oscillatory behavior shows that the probability of the emission events is affected by the interference between the waves generated by the individual cavities. The dashed curve in Fig. 3(a) represents a simple fit to the anomalous emission rate,  $\Gamma_N \delta x \approx A \cos^2 \delta 2kd$  for  $A \approx 1.36$ , and  $k \approx 2\pi/\lambda$ , with  $\lambda \approx 6.60 \pm 0.05 \text{ mm}$  being the experimentally measured wavelength of the Faraday waves in the vicinity of the cavities (Fig. 2). Owing to experimental limitations, we did not systematically characterize the decay of the anomalous emission rate with increasing separation distance  $d$ . Nevertheless, we note that the influence of the neighboring cavity’s wave field will decay with  $d$  due to viscous damping, as will the anomalous emission rate.

Figure 3(b) depicts the time dependence of the emission events from a single cavity, showing the unpredictability of a single emission event, as is confirmed by the FFT analysis presented in the Supplemental Material [31]. While the highly nonlinear and chaotic nature of the emission events makes theoretical or numerical modeling of the emission phenomenon a daunting task, we proceed by demonstrating that the problem lends itself to a stochastic approach. Let  $X_t$  be a stochastic process representing the maximal wave field amplitude inside the cavities, with  $X_0 \approx 0$  representing the initially flat state. Between two consecutive emission events, we assume that the maximal wave field amplitude oscillates stochastically about some mean value  $\mu \delta t$  that grows in time as a result of the resonant interaction between the external forcing and the cavities. Eventually, the maximal amplitude crosses a threshold  $\alpha$ , resulting in an emission of a droplet, after which  $X_t$  relaxes back to  $X_0 \approx 0$  and the process starts over. Thus, one may write

$$X_t \approx vt + \sigma W_t; \quad v, \sigma > 0 \quad \delta t$$

where  $vt$  is a stochastic drift representing the increase in  $\mu \delta t$  between consecutive emission events, and  $W_t$  is a Wiener process with an amplitude  $\sigma$ , representing the stochastic oscillations of  $X_t$  about  $\mu \delta t$ . The emission process can thus be modeled as a first passage time problem, where we seek to find the first time that  $X_t$  reaches the critical value  $\alpha$ , at which point an emission event occurs. For a Wiener process with a stochastic drift, the probability density function for the first passage time is given by the inverse Gaussian distribution [36]

$$P(\delta T_\alpha) \approx \frac{\kappa}{2\pi T_\alpha^3} \exp\left(-\frac{\kappa \delta T_\alpha - \mu \delta T_\alpha^2}{2\mu^2 T_\alpha}\right) \quad \delta T_\alpha$$

where  $T_\alpha$  is the first time  $X_t$  crosses the threshold value  $\alpha$ ,  $\kappa \approx \delta \alpha = \sigma \mu$  is the shape parameter, and  $\mu \approx \delta \alpha = v \mu$  is the mean value of  $T_\alpha$ . Figure 3(c) presents a histogram of the

experimentally measured interemission time intervals for the case  $d \approx 12$  mm, which shows good agreement with Eq. (2) when  $\kappa \approx 3.3$  is used for the shape parameter.

The mechanism responsible for the superradiant emission of droplets is the wave coupling between the two cavities. We quantify this coupling by measuring the correlations between the emission events in the two-cavity system, as detailed in the Supplemental Material [31]. We see that the two cavities are strongly anticorrelated, with the correlation values varying from  $C \approx -0.30$  (for  $d \approx 11.5$  mm) to  $C \approx -0.41$  (for  $d \approx 10$  mm). Figure 4 shows the measured correlation  $C$  of the drop emission event in the two cavities as a function of their separation distance  $d$ . Presumably, the anticorrelation arises because each time a droplet is emitted, a small amount of liquid is removed from the system for a brief period of time, leading to a diminution in the probability of another ejection. The emission of one droplet serves to delay the emission of the next.

These anticorrelations, together with the amplification of the combined emission rate, suggest that the two-cavity system cannot be factored into distinct states, as the probabilities of emission events in the two cavities are coupled. Acting on one of the cavities of this coupled system, by, for example, changing its position or depth, would affect the emission rate of its neighboring cavity. The possibility thus arises of altering the system's global emission rate by a local operation on one of its individual components, thereby creating a new platform for probabilistic computational operations in fluid mechanics.

It is also worth considering the relation between the system introduced here and pilot-wave hydrodynamics [24,37]. In the latter, the notion of an analog photon is more nebulous: when the system jumps between quantized states (e.g., the walking droplet transitions from one orbit to another, or tunnels between two energetically distinguishable cavities [37]), energy is dumped into or extracted from the bath. In the system considered here, droplets are generated by breaking waves, their appearance representing a discrete transition event, an analog of photon emission from an excited state. We note that in our current experiments, we used fluorinated oil in order to facilitate the rapid reabsorption of the emitted droplets into the bath. However, this reabsorption can be minimized by using a relatively low density silicon oil, in which case the generated particles may persist on the surface, bounce, and self-propel, thereby providing a possible link between pilot-wave hydrodynamics and the new class of analog systems established here.

We proceed by enumerating several notable differences between optical superradiance and our hydrodynamic analogy. First, in our experiments we did not characterize the structure of the energy levels as would potentially be prescribed by the size and kinetic energy of the emitted droplets, or the transition rates associated with these levels, both of which are well characterized in the quantum mechanical system. Second, in our experiments we did not observe subradiant droplet emission. We believe that

the latter is due to the chosen cavity geometry precluding the possibility of robust destructive interference. Specifically, in order to support a single oscillatory mode in each cavity, the liquid bath would need to be strongly driven at a frequency on the order of 10 Hz, which was unreachable with our current setup. Driving the system at 39 Hz excited higher harmonics inside the cavities, yielding a complex 2D wave field which could not be canceled by the ordered wave field in the shallow intercavity region. We note that in the optical case, while superradiance is readily observed in a wide variety of systems, subradiance is very difficult to obtain [13,38].

Another comparison can be made between the generation of droplets in our hydrodynamic system and the emission of photons in its optical counterpart. Both processes represent dissipative mechanisms, the rates of which depend nonlinearly on the amplitude of the relevant field. In the hydrodynamic case, the probability of random discrete events, specifically drop ejection, is prescribed by a continuous wave field resulting from two interfering sources. This statistical behavior is reminiscent of the way probabilities of outcomes are obtained from Born's rule in the standard quantum theory.

We have introduced a new hydrodynamic system that shares several key features with the phenomenon of superradiance in optics. In addition to the amplification of the emission rate typically associated with superradiance, our system exhibits sinusoidal dependence of the amplified emission rate on separation distance [see Fig. 3(b)], as arises from classical wave interference. Finally, our study suggests that droplet creation through interfacial fracture may provide a valuable new platform for exploring hydrodynamic analogs of particle emission phenomena, and so further extend the range of hydrodynamic quantum analogs.

We thank Masha Bluvshstein for her help with analyzing the data, and Christos Orestis Apostolidis for providing the graphical schematics used in this Letter. We also thank Matthieu Labousse and André Nachbin for valuable discussions, as well as Shimon Rubin and Tal Kachman for their constructive comments on the manuscript. We also gratefully acknowledge the financial support of the United States Department of State (V.F.), the European Union's Horizon 2020 research and innovation program under the Marie Skłodowska-Curie project EnHydro, Grant Agreement No. 841417 (K.P.), and the National Science Foundation Grant No. CMMI-1727565 (J.B.).

The authors declare no competing interests.

\*These authors contributed equally to this work.

†bush@math.mit.edu

- [1] W. Zakowicz and K. Rzazewski, Collective radiation by harmonic oscillators, *J. Phys. A* **7**, 869 (1974).
- [2] I. Tralle and P. Zieba, Induced N<sub>2</sub>-cooperative phenomenon in an ensemble of the nonlinear coupled oscillators, *Phys. Lett. A* **378**, 1364 (2014).

- [3] R. H. Dicke, Coherence in Spontaneous Radiation Processes, *Phys. Rev.* **93**, 99 (1954).
- [4] A. Kalachev, Quantum storage on subradiant states in an extended atomic ensemble, *Phys. Rev. A* **76**, 043812 (2007).
- [5] A. T. Black, J. K. Thompson, and V. Vuletić, On-Demand Superradiant Conversion of Atomic Spin Gratings into Single Photons with High Efficiency, *Phys. Rev. Lett.* **95**, 133601 (2005).
- [6] M. O. Scully, Single Photon Subradiance: Quantum Control of Spontaneous Emission and Ultrafast Readout, *Phys. Rev. Lett.* **115**, 243602 (2015).
- [7] A. K. Ekert, Quantum Cryptography Based on Bell's Theorem, *Phys. Rev. Lett.* **67**, 661 (1991).
- [8] D. Meiser, J. Ye, D. R. Carlson, and M. J. Holland, Prospects for a Millihertz-Linewidth Laser, *Phys. Rev. Lett.* **102**, 163601 (2009).
- [9] J. G. Bohnet, Z. Chen, J. M. Weiner, D. Meiser, M. J. Holland, and J. K. Thompson, A steady-state superradiant laser with less than one intracavity photon, *Nature (London)* **484**, 78 (2012).
- [10] A. A. Svidzinsky, L. Yuan, and M. O. Scully, Quantum Amplification by Superradiant Emission of Radiation, *Phys. Rev. X* **3**, 041001 (2013).
- [11] M. O. Scully and A. A. Svidzinsky, The super of super-radiance, *Science* **325**, 1510 (2009).
- [12] M. Gross and S. Haroche, Superradiance: An essay on the theory of collective spontaneous emission, *Phys. Rep.* **93**, 301 (1982).
- [13] P. Solano, P. Barberis-Blostein, F. K. Fatemi, L. A. Orozco, and S. L. Rolston, Super-radiance reveals infinite-range dipole interactions through a nanofiber, *Nat. Commun.* **8**, 1857 (2017).
- [14] E. A. Power, Effect on the lifetime of an atom undergoing a dipole transition due to the presence of a resonating atom, *J. Chem. Phys.* **46**, 4297 (1967).
- [15] R. G. DeVoe and R. G. Brewer, Observation of Superradiant and Subradiant Spontaneous Emission of Two Trapped Ions, *Phys. Rev. Lett.* **76**, 2049 (1996).
- [16] A. A. Makarov and V. S. Letokhov, Spontaneous decay in a system of two spatially separated atoms (One-dimensional case), *J. Exp. Theor. Phys.* **97**, 688 (2003).
- [17] H. Tanji-Suzuki, I. D. Leroux, M. H. Schleier-Smith, M. Cetina, A. T. Grier, J. Simon, and V. Vuletić, Chapter 4—Interaction between Atomic Ensembles and Optical Resonators: Classical Description, in *Advances In Atomic, Molecular, and Optical Physics*, edited by E. Arimondo, P. R. Berman, and C. C. Lin, *Advances in Atomic, Molecular, and Optical Physics Vol. 60* (Academic Press, New York, 2011), pp. 201–237.
- [18] T. Young, I. The Bakerian Lecture. Experiments and calculations relative to physical optics, *Phil. Trans. R. Soc. London* **94**, 1 (1804).
- [19] W. G. Unruh, Experimental Black-Hole Evaporation?, *Phys. Rev. Lett.* **46**, 1351 (1981).
- [20] B. C. Denardo, J. J. Puda, and A. Larraza, A water wave analog of the Casimir effect, *Am. J. Phys.* **77**, 1095 (2009).
- [21] M. V. Berry, R. G. Chambers, M. D. Large, C. Upstill, and J. C. Walmsley, Wavefront dislocations in the Aharonov-Bohm effect and its water wave analogue, *Eur. J. Phys.* **1**, 154 (1980).
- [22] P. H. Steen, C.-T. Chang, and J. B. Bostwick, Droplet motions fill a periodic table, *Proc. Natl. Acad. Sci. U.S.A.* **116**, 4849 (2019).
- [23] Y. Couder and E. Fort, Single-Particle Diffraction and Interference at a Macroscopic Scale, *Phys. Rev. Lett.* **97**, 154101 (2006).
- [24] J. W. M. Bush and A. U. Oza, Hydrodynamic quantum analogs, *Rep. Prog. Phys.* **84**, 017001 (2020).
- [25] E. Fort, A. Eddi, A. Boudaoud, J. Moukhtar, and Y. Couder, Path-memory induced quantization of classical orbits, *Proc. Natl. Acad. Sci. U.S.A.* **107**, 17515 (2010).
- [26] S. Perrard, M. Labousse, M. Miskin, E. Fort, and Y. Couder, Self-organization into quantized eigenstates of a classical wave-driven particle, *Nat. Commun.* **5**, 3219 (2014).
- [27] D. M. Harris, J. Moukhtar, E. Fort, Y. Couder, and J. W. M. Bush, Wavelike statistics from pilot-wave dynamics in a circular corral, *Phys. Rev. E* **88**, 011001(R) (2013).
- [28] P. J. Sáenz, T. Cristea-Platon, and J. W. M. Bush, Statistical projection effects in a hydrodynamic pilot-wave system, *Nat. Phys.* **14**, 315 (2018).
- [29] P. J. Sáenz, T. Cristea-Platon, and J. W. M. Bush, A hydrodynamic analog of Friedel oscillations, *Sci. Adv.* **6**, eaay9234 (2020).
- [30] P. J. Sáenz, G. Pucci, S. E. Turton, A. Goujon, R. R. Rosales, J. Dunkel, and J. W. M. Bush, Emergent order in hydrodynamic spin lattices, *Nature (London)* **596**, 58 (2021).
- [31] See Supplemental Material at <http://link.aps.org/supplemental/10.1103/PhysRevLett.130.064002> for details on materials and methods, unpredictability of emission events, and inter-cavity coupling.
- [32] D. M. Harris and J. W. M. Bush, Generating uniaxial vibration with an electrodynamic shaker and external air bearing, *J. Sound Vib.* **334**, 255 (2015).
- [33] M. Faraday, On a peculiar class of acoustical figures; and on certain forms assumed by groups of particles upon vibrating elastic surfaces, *Phil. Trans. R. Soc. London* **3**, 49 (1837).
- [34] C. L. Goodridge, W. T. Shi, H. G. E. Hentschel, and D. P. Lathrop, Viscous effects in droplet-ejecting capillary waves, *Phys. Rev. E* **56**, 472 (1997).
- [35] C. L. Goodridge, H. G. E. Hentschel, and D. P. Lathrop, Breaking Faraday Waves: Critical Slowing of Droplet Ejection Rates, *Phys. Rev. Lett.* **82**, 3062 (1999).
- [36] J. L. Folks and R. S. Chhikara, The inverse Gaussian distribution and its statistical application—a review, *J. R. Stat. Soc.* **40**, 263 (1978).
- [37] K. Papatryfonos, M. Ruelle, C. Bourdiol, A. Nachbin, J. W. M. Bush, and M. Labousse, Hydrodynamic super-radiance in wave-mediated cooperative tunneling, *Commun. Phys.* **5**, 142 (2022).
- [38] W. Guerin, M. O. Araújo, and R. Kaiser, Subradiance in a Large Cloud of Cold Atoms, *Phys. Rev. Lett.* **116**, 083601 (2016).